Technical Physics, 2023, Vol. 68, No. 12

Mechanical properties of porous titanium nickelide with different spatial pore distribution under uniaxial tension

© G.A. Nikiforov, B.N. Galimzyanov, A.V. Mokshin

Kazan Federal University,
420008 Kazan, Russia
e-mail: nikiforov121998@mail.ru

Received May 19, 2023
Revised June 16, 2023
Accepted October, 30, 2023

A model of nanoporous titanium nickelide is constructed, where the distribution of the thickness of the interpore bridges is qualitatively similar to the same distribution in experimentally obtained millimeter-sized samples. It is shown that the tensile strength of porous samples with a uniform density profile of a solid matrix is approximately 1.5 times greater and the Young's modulus is approximately 1.3 times greater than that of samples with an uneven profile.

Keywords: porous titanium nickelide, mechanical properties, morphology of the porous structure.

DOI: 10.61011/TP.2023.12.57722.f217-23

Introduction

Titanium nickelide intermetallic $Ni_{50}Ti_{50}$ has unique properties such as shape memory effect, superelasticity and biocompatibility [1,2]. At the same time, porous titanium nickelide is actively used for the manufacture of implants [3]. The unique functional properties of titanium nickelide are due to a phase transition of the first kind, called martensitic transformation [4]. The martensitic transformation is realized in the temperature range $300-380$ K and can be initiated by the deformation [5,6]. It should be noted that methods of improving mechanical characteristics, such as alloying, can negatively affect the realization of the functional properties of the material, reducing the concentration of phases that realize the martensitic transformation [7]. We suggest that the mechanical properties should be improved by achieving a uniform distribution of the crystal matrix in the direction of the load.

1. Simulation details

The dynamics simulation of atoms in crystalline titanium nickelide is carried out for a system in the B2 phase with a total number of atoms $\approx 25\,000$. In the equilibrium state, the porous system reaches a size of 9 nm with pore sizes of the order of $4-5$ nm and porosity $\approx 55\%$. The porous system was produced by removing atoms from a crystalline base. In contrast to the production of a porous system by rapid melt cooling [8,9], the method used in this paper allows the crystal structure of the material to be preserved. The interatomic interaction is given by the potential 2NN MEAM [10]:

$$E = \sum_i \left[F_i(\rho_i) + \frac{1}{2} \sum_{i \neq j} S_{ij} \phi_{ij}(R_{ij}) \right].$$

In this expression, E — total energy of the system; $F_i(\rho_i)$ — energy „of the immersed atom", which depends on the electron density; $S_{ij}\phi_{ij}(R_{ij})$ — functions of the pairwise interaction of atoms, which depend on the distance between the particles. It should be noted that this potential reproduces well the structure and physical and mechanical properties of nitinol for a wide thermodynamic domain, as shown earlier in the papers [11–13].

In this paper, samples of porous nitinol with an uneven density profile $L(x)$ of a solid crystal matrix, as well as samples with a relatively uniform density profile along the x axis, were prepared. Samples with a uniform density profile were obtained by adjusting the position of the pores so that the density profile varied slightly along the stretch axis (Fig. 1, *b*). We note that the density profile is not uniform along the other directions. The stretching took place at a temperature of 300 K with a strain rate $\dot{\varepsilon} = 5 \cdot 10^9\,\mathrm{s}^{-1}$ in the NVT ensemble. This strain rate is typical for molecular dynamics simulation, as the typical simulation time scale is of the order of 100 ps.

2. Discussion

The thickness distributions of the interpore bridges were calculated and presented in comparison with the experimental distribution for porous titanium nickelide with an average pore size $90\,\mu$m [14] (Fig. 2). It is important to note that the bridge thicknesses were normalized to the mean bridge thickness ($\bar{l}_{MD} \approx 2.8$ nm and $\bar{l}_{\exp} \approx 127\,\mu$m), and the distribution of pore thicknesses to dimensions was normalized as $\int P(l)dl = 1$. From Fig. 2 it can be seen that the thickness distribution of the interpore bridges in the case of a system with an uneven density profile qualitatively repeats the distribution obtained from the experiment. In turn, the shift of the distribution towards larger bridge thicknesses in the case of a uniform density profile leads to improved mechanical properties.

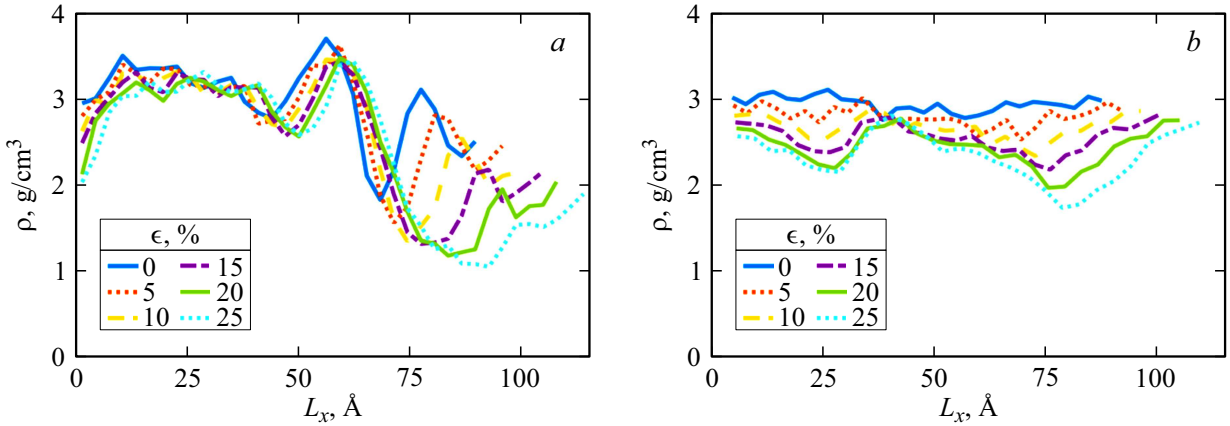

Figure 1. Tensile density profiles for a specimen with a non-uniform density profile (a) and a uniform density profile (b). Here ε — relative deformation of the specimen.

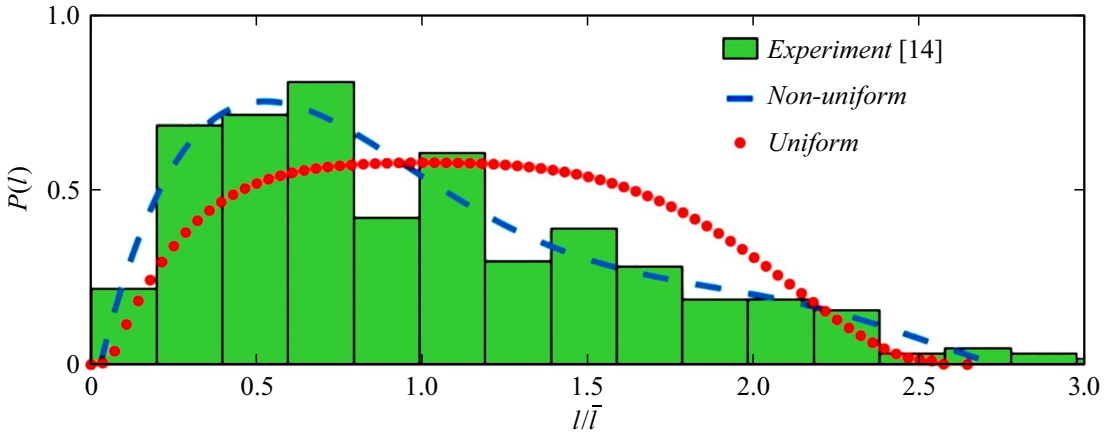

Figure 2. Comparison of thickness distributions of interpore bridges normalized to mean bridge thickness.

Stretching the specimens in question allowed us to detect different fracture behavior of the specimens depending on the morphology of the porous system. From Fig. 1, a it can be seen that the non-uniform density profile is characterized by the presence of pronounced extremes with alternating minima and maxima. Due to the presence of such extremes, the rigid matrix distributes the loads caused by tension unevenly. Therefore, the tensile collapse of the system begins near the region with the lowest density. The position and depth of the global minimum can be easily detected from the density profile graph (Fig. 1, a). For comparison, in the case of a porous system with a relatively uniform density profile, there are several minima of the same depth, as can be clearly seen from the figure (Fig. 1, b). Fig. 1, b shows that in the case of a system with a relatively uniform density profile, the formation of a stable global minimum occurs only at deformations of 15%. In this way, the system distributes the load much more efficiently and resists destruction for much longer.

From the resulting strain stress curve—shown in Fig. 3, it follows that a specimen with a uniform density profile has increased strength characteristics compared to a specimen with an uneven density profile in the case of uniaxial tension. This is confirmed by the calculated value of the tensile strength $\sigma_{frac} \approx 1.8 \pm 0.2$ GPa at deformation 20%, which is 1.5 times the tensile strength of the specimen with an uneven density profile ($\sigma_{frac} = 1.2 \pm 0.2$ GPa at deformation 17.5%). In this case, the Young's modulus E of samples with a uniform density profile is $E \approx 20.0 \pm 0.5$ GPa, while for samples with a non-uniform density profile $E \approx 14.9 \pm 0.2$ GPa.

Conclusion

The results of this study showed that porous nitinol with a uniform density profile has increased strength characteristics under uniaxial tension. Such a profile means that the density of the solid matrix remains constant (or changes slightly) in the direction of the tensile force. This results in a more uniform distribution of the load within the system and thus an increase in tensile strength and ultimate deformation. We have showed that the tensile strength of porous nitinol with a uniform density profile of the

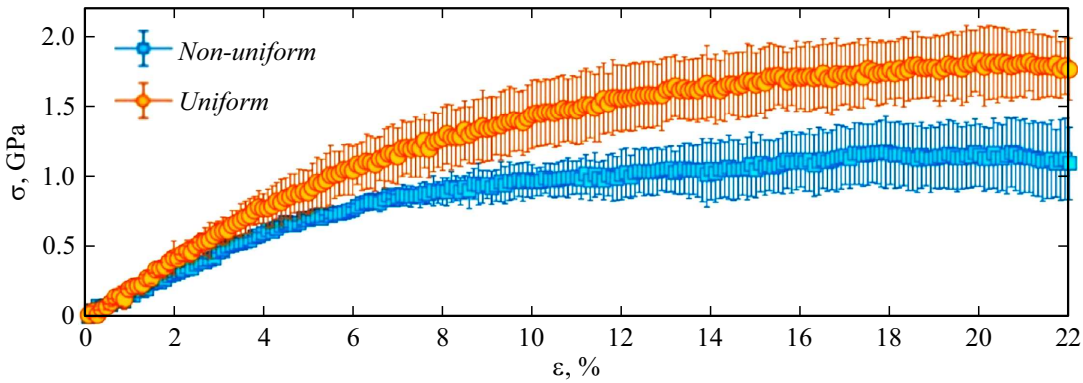

Figure 3. Stress curves–strain for specimens with uniform and non-uniform density profiles.

crystal matrix is 1.5 times greater than that of samples with an uneven profile. Therefore, porous metal alloys with a uniform density profile pertain to the materials with improved performance properties.

Funding

This study was performed as part of the Program „Priority — 2030".

Conflict of interest

The authors declare that they have no conflict of interest.

References

[1] T. Duerig, A. Pelton, D. Stöckel. Mater. Sci. Eng., **273**, 149 (1999). DOI: 10.1016/S0921-5093(99)00294-4
[2] D. Kapoor. Johnson Matthey Technol. Rev., **61** (1), 66 (2017). DOI: 10.1595/205651317X694524
[3] S.A. Shabalovskaya. Bio-Medical Mater. Eng., **12** (1), 69 (2002).
[4] D.J. Hartl, D.C. Lagoudas. Proc. IMechE Part G: J. Aerospace Eng., **221** (4), 540 (2007). DOI: 10.1243/09544100JAERO211
[5] H. Aihara, J. Zider, G. Fanton, T. Duerig. Interna. J. Biomater., **2019** (4307461), 1 (2019). DOI: 10.1155/2019/4307461
[6] S. Daly, G. Ravichandran, K. Bhattacharya. Acta Mater., **55** (10), 3593 (2007). DOI: 10.1016/j.actamat.2007.02.011
[7] A.N. Monogenov, E.S. Marchenkoa, G.A. Baigonakova, Y.F. Yasenchuk, A.S. Garin, A.A. Volinsky. J. Alloys Comp., **918** (165617), 10 (2022). DOI: 10.1016/j.jallcom.2022.165617
[8] B.N. Galimzyanov, G.A. Nikiforov, A.V. Mokshin. Acta Phys. Polonica A., **137**, 1149 (2020). DOI: 10.12693/APhysPolA.137.1149
[9] G.A. Nikiforov, B.N. Galimzyanov, A.V. Mokshin. UZFF MGU, **2019** (4), 1940703 1 (2019).
[10] W.-S. Ko, B. Grabowski, J. Neugebauer. Phys. Rev. B., **92** (134107), 1 (2015). DOI: 10.1103/PhysRevB.92.134107
[11] J. Chen, D. Huo, H.K. Yeddu. Mater. Res. Express, **8** (106508), 1 (2021). DOI: 10.1088/2053-1591/ac2b57
[12] J. Lee, Y.C. Shin. Metals, **11**, 1237 (2021). DOI: 10.3390/met11081237
[13] Y. Guo, X. Zeng, H. Chen, T. Han, H. Tian, F. Wang. Adv. Mater. Sci. Eng., 1 (2017). DOI: 10.1155/2017/7427039
[14] V.N. Khodorenko, S.G. Anikeev, V.É. Gunther. Rus. Phys. J., **57** (6), 726 (2014). DOI: 10.1007/s11182-014-0296-5

Translated by 123